MOLECULAR AND CELLULAR BIOLOGY, June 2008, p. 3790–3803 Vol. 28, No. 11
0270-7306/08/$08.00+0 doi:10.1128/MCB.01580-07

Hypoxia-Inducible Factor-Dependent Degeneration, Failure, and Malignant Transformation of the Heart in the Absence of the von Hippel-Lindau Protein▽

Li Lei,[1] Steve Mason,[2] Dinggang Liu,[1] Yan Huang,[1] Carolyn Marks,[3] Reed Hickey,[1] Ion S. Jovin,[1] Marc Pypaert,[3] Randall S. Johnson,[2] and Frank J. Giordano[1]*

Cardiovascular Gene Therapy Program, Department of Medicine, Yale University School of Medicine, New Haven, Connecticut 06510[1]; Department of Biology, University of California San Diego, La Jolla, California[2]; and Electron Microscopy Core, Department of Cell Biology, Yale University School of Medicine, New Haven, Connecticut 06510[3]

Received 28 August 2007/Returned for modification 1 October 2007/Accepted 7 February 2008

Hypoxia-inducible transcription factor 1 (HIF-1) and HIF-2α regulate the expression of an expansive array of genes associated with cellular responses to hypoxia. Although HIF-regulated genes mediate crucial beneficial short-term biological adaptations, we hypothesized that chronic activation of the HIF pathway in cardiac muscle, as occurs in advanced ischemic heart disease, is detrimental. We generated mice with cardiac myocyte-specific deletion of the von Hippel-Lindau protein (VHL), an essential component of an E3 ubiquitin ligase responsible for suppressing HIF levels during normoxia. These mice were born at expected frequency and thrived until after 3 months postbirth, when they developed severe progressive heart failure and premature death. VHL-null hearts developed lipid accumulation, myofibril rarefaction, altered nuclear morphology, myocyte loss, and fibrosis, features seen for various forms of human heart failure. Further, nearly 50% of $VHL^{-/-}$ hearts developed malignant cardiac tumors with features of rhabdomyosarcoma and the capacity to metastasize. As compelling evidence for the mechanistic contribution of HIF-1α, the concomitant deletion of VHL and HIF-1α in the heart prevented this phenotype and restored normal longevity. These findings strongly suggest that chronic activation of the HIF pathway in ischemic hearts is maladaptive and contributes to cardiac degeneration and progression to heart failure.

In the cardiovascular system, hypoxia is encountered in a number of important clinical settings, including sleep apnea, chronic obstructive pulmonary disease, and, most commonly, ischemic heart disease (IHD). Myocardial hypoxia, as a component of ischemia, may also occur in other common clinical conditions, such as valve disease, pathological cardiac hypertrophy, and severe systemic hypertension. As such, understanding how hypoxia-induced molecular changes affect the heart is of great importance. Altered gene expression mediated by hypoxia-inducible transcription factor 1α (HIF-1α) and HIF-2α is one of the most fundamental and ubiquitous mechanisms whereby biological adaptations to hypoxia occur. The HIFs are basic helix-loop-helix transcription factors that regulate the expression of a wide repertoire of genes involved in a myriad of biological functions, including angiogenesis, apoptosis, and cellular metabolism (14, 17, 51). A third family member, HIF-3α, lacks a transcriptional activation domain and may act as a competitive inhibitor of HIF-1α and -2α activity (41).

Although HIF-1α and -2α appear to bind the same hypoxia response elements (HREs) in hypoxia-inducible genes, it has been established that they preferentially regulate different genes in different cell types and therefore are not redundant. The role of HIF-1α in the transcriptional control of angiogenesis has led to the ongoing development of HIF-1α as a therapeutic stimulator of angiogenesis in IHD and peripheral vascular disease (12, 15, 48, 60), although clinical development of HIF-2α for this purpose has also been considered. Others and we have previously shown that HIF-1α plays a cardioprotective role and is essential for the maintenance of normal cardiac function and gene expression, even under normoxic conditions (7, 23). Thus, the role of HIF-1α in the heart has been established as beneficial and adaptive. However, the effects of chronic activation of the endogenous HIF pathway in the heart, as can occur in advanced IHD, to date have remained unclear.

Regulation of the HIF pathway is complex, and understanding HIF regulation is essential to any approach designed to model the effects of chronic HIF pathway activation. The major level of HIF regulation is posttranslational, involving the von Hippel-Lindau protein (VHL) and the ubiquitin-proteosome degradation pathway (14, 52). Consequently, simple transcriptional overexpression of wild-type HIF-1 or -2α can fail to raise HIF levels commensurate with what is encountered normally during hypoxia. In the context of clinical development, this was addressed by removing the degron domain and replacing it with the VP16 transactivation domain (48). It is possible that by altering the C termini of HIF proteins to achieve stability of overexpression, the repertoire of biological activities of HIF could be altered. Therefore, to study chronic HIF pathway activation we deleted the VHL gene. VHL is an ~30-kDa protein that functions as a major subunit in an E3

* Corresponding author. Mailing address: Cardiovascular Gene Therapy Program, Department of Medicine, Yale University School of Medicine, BCMM 436C, 295 Congress Avenue, New Haven, CT 06510. Phone: (203) 785-7631. Fax: (203) 737-2290. E-mail: frank.giordano@yale.edu.

▽ Published ahead of print on 19 February 2008.

ubiquitin ligase complex (38, 47, 50). Other biological functions have been ascribed to VHL (3), but its role in the ubiquitylation of HIF-1α and -2α is the best established (25, 26, 37, 62). Under normoxic conditions, HIF-1α and its cousins HIF-2 and -3α undergo prolyl hydroxylation, an event that promotes VHL binding and the ubiquitylation of HIF (52). This polyubiquitylation results in the degradation of HIF in the proteosome; thus, VHL is a negative regulator of HIF protein levels. Mutation or loss of a single VHL allele is associated with von Hippel-Lindau syndrome, characterized by central nervous system and retinal hemangioblastomas, renal and epididymal cysts, pheochromocytoma, and an increased risk of developing renal cell carcinoma (38, 50). Each of these has been postulated to be related to chronic HIF pathway activation, including HIF-induced angiogenesis in the genesis of hemangioblastomas, HIF-mediated overexpression of tyrosine hydroxylase in pheochromocytoma, and HIF-mediated expression of transforming growth factor alpha (TGF-α) in renal cell carcinoma. Although biallelic silencing of VHL does occur secondary to spontaneous somatic mutation or promoter hypermethylation, global homozygous VHL mutations in patients have not been described (33, 34). In addition, no cardiospecific role of VHL has been previously delineated.

In this report we show that the absence of VHL in heart muscle causes lipid accumulation, myofibrillar rarefaction and disarray, profound nuclear envelope and nuclear architecture abnormalities, cardiac muscle degeneration and loss, increased autophagy, and the development of severe heart failure. We further show that the loss of VHL allows cardiac dedifferentiation and the development of malignant cardiac tumors exhibiting features of rhabdomyosarcoma and the capacity to metastasize. Finally, by generating mice with combined deletion of VHL and HIF-1α specifically in cardiac muscle, we demonstrate that the profound cardiac abnormalities that occur as a consequence of VHL deletion do not occur in the absence of HIF-1α, establishing that the chronic activation of a HIF-1α-dependent gene program is markedly deleterious in the heart.

MATERIALS AND METHODS

Generation of cardiac myocyte-specific VHL$^{-/-}$ mice. MLC2v-Cre haploid knock-in mice were crossed with VHL$^{loxP/loxP}$ mice (Vhlh$^{tm1Jae/J}$ strain; Jackson Labs) that harbor loxP sites flanking the promoter and exon 1 of the VHL gene (22). Both lines were back-bred for at least six generations into a C57BL/6 background. Genotyping and gene frequency analysis were performed using VHL-specific primers and a standard PCR method on tail-derived DNA as previously described (13, 23). Mice with homozygous cardiac myocyte-specific deletion of VHL (Cre$^{+/-}$ VHL$^{loxP+/+}$) were designated cmVHL$^{-/-}$. For all studies, results are from cmVHL$^{-/-}$ mice and their age-matched, gender-matched VHL$^{+/+}$ littermates (controls were Cre$^{-/-}$ × VHL$^{loxP+/+}$ and are designated cmVHL$^{+/+}$). The MLC2v-Cre mice were created by knock-in of Cre downstream of the MLC2v promoter. These mice have no basal or inducible phenotype, have normal levels of MLC2v protein expression despite being haploid for the MLC2v gene, and are a well-established cardiac myocyte-directed Cre line (5, 16, 23, 42).

Immunohistochemistry, histology, and transmission EM. For standard histology, hearts were fixed in formalin, embedded in paraffin, sectioned, and stained (hematoxylin and eosin, lipid O red, trichrome) by the Yale Pathology core facility. For immunohistochemistry, OCT-embedded frozen sections were used. Five-micrometer sections were cut and fixed with acetone-methanol. A monoclonal anti-PECAM antibody (Invitrogen, San Diego, CA) was used for microvessel counts. Four VHL$^{-/-}$ and four littermate control hearts were sectioned, and digital images from five separate 40× fields were assessed from each section as described previously. Vessel density was also analyzed by Western blotting for PECAM and Flt-1 on protein lysates from VHL$^{-/-}$ and control hearts. Vascular casts were created by infusing Microfil polymer into the coronary tree via retrograde aortic perfusion at constant pressure, as we have previously described (16). For transmission electron microscopy (EM), hearts were fixed by retrograde perfusion with a buffered solution containing 2% EM-grade glutaraldehyde. Subsequent processing was done at the Yale EM core.

Echocardiography. Echocardiograms were obtained for lightly anesthetized mice (isofluorane inhalation) by use of a 15-MHz transducer and a Sonos 7500 console as previously described (13, 23). Zoomed two-dimensional views were used to determine a short-axis plane at the level of the papillary muscles, and then M-mode was obtained at this level. Measurements were obtained using the 7500 analysis software.

Tumor cell culture, soft agarose assay, in vivo tumor assay. Cells were disaggregated from excised tumors by a short (10- to 15-min) incubation with type I collagenase (Worthington, Inc.). Cells were initially cultured in Dulbecco modified Eagle medium-20% fetal bovine serum, with serum levels decreased sequentially upon serial passage. For analysis of anchorage-independent growth, a standard soft agar assay was used in which cells were suspended in 1 ml of 0.3% agar (Difco) supplemented with complete growth medium. The agar was allowed to gel at room temperature over a 0.8-ml base layer of growth medium-supplemented 0.6% agar in six-well plates ($n \geq 3$ gels/condition). Colony formation was determined by light microscopy and compared to a positive control (HepG2 cells) and nontransformed negative control cells (h9c2 cells) (HepG2 and h9c2 cells were obtained from the ATCC). In vivo tumor formation was assessed as previously described by subcutaneous injection of 5×10^6 tumor cells in Rag2$^{-/-}$ (Taconic, Inc., NY) immune-deficient mice and compared to what was seen for control injections of nontransformed cells (20).

In vivo gene delivery. Recombinant adenoviruses encoding HIF-1α with the degron transactivation domain replaced by the VP16 transactivation domain, wild-type HIF-1α, and beta-galactosidase were constructed and expanded as previously described (18). Day 1 neonatal mice were anesthetized by ice immersion and adenoviral gene delivery to the heart was achieved using 10-μl glass capillary tubes pulled to a point to create pipettes. These were filled with 10 μl of adenovirus containing ~1×10^9 viral particles. By use of a micromanipulator, the pipette tip was inserted into the heart directly through the chest wall and the adenovirus was then injected, as previously reported (6).

Gene expression, floxing efficiency, and quantification of mitochondrial DNA. For real-time reverse transcriptase PCR (RT-PCR), total RNA was extracted from the left ventricles of VHL$^{-/-}$ and littermate control mice by use of RNA Stat-60 reagent (Tel-Test, Inc.), treated with RNase-free DNase I (Roche), and column purified (Qiagen). RT-PCR was performed in two steps. First-strand cDNA was synthesized with the ProSTAR first-strand RT-PCR kit (Stratagene) by use of random primers. Conditions for the RT reactions were 1 h at 42°C and 10 min at 95°C. SYBR green JumpStart *Taq* ReadyMix (Sigma) was used in the second step of real-time PCR amplification of first-strand cDNA. Reactions were run in 96-well plates on an Opticon-2 quantitative PCR block (MJ Research, Inc.). For all primer pairs, the presence of a single gene product was verified by agarose gel electrophoresis. Melting curves were also examined after each run. For Western blot analysis, equally loaded protein samples underwent electrophoresis on 10% NuPAGE gels (Invitrogen, San Diego, CA). Protein bands were transferred onto nitrocellulose membranes and blocked with 5% nonfat milk. Membranes were incubated at 4°C overnight with primary antibody, washed and incubated for 1 h with secondary antibody, and developed using chemiluminescence.

For determination of floxing efficiency, genomic DNA was isolated from cardiac myocytes and nonmyocytes isolated from knockout and control hearts. Quantitative PCR was performed using a primer pair designed to give product only in the absence of floxing. Quantification of mitochondrial DNA was performed by quantitative PCR using the following primers: F, 5′-GCCCCAGAT ATAGCATTCCC-3′; and R, 5′-GTTCATCCTGTTCCTGCTCC-3′.

Ras activation and HIF activity assays. Ras activation was assessed using a commercial assay kit (Upstate Inc., Waltham, MA). Briefly, this assay pulls down activated Ras onto Raf1 agarose and quantitates this activated Ras by subsequent Western blot analysis. The activity of HIF-1α was determined using a commercial DNA-binding enzyme-linked immunosorbent assay (ELISA)-based kit that binds HIF-1α from the samples onto plated oligonucleotides that contain HIF HREs and then uses an anti-HIF antibody for quantitation of bound HIF-1α (TransAM; ActiveMotif, Carlsbad, CA). The validity of the assay was verified using control HIF-1α peptide and mutant peptide in competition assays.

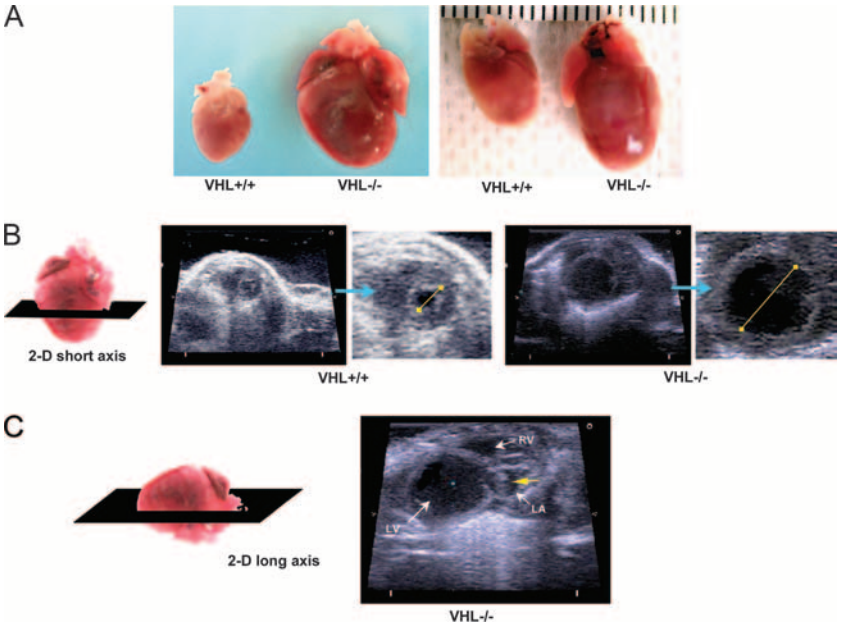

FIG. 1. Targeted deletion of VHL in cardiac myocytes leads to cardiomegaly, progressive heart failure, tumor formation, and cardiac death. (A) Cardiac myocyte-specific deletion of VHL ($VHL^{-/-}$) results in development of severe cardiomegaly relative to what is seen for hearts from age- and sex-matched littermates ($VHL^{+/+}$). (B) Short-axis two-dimensional (2-D) echocardiography (orientation of ultrasound slice depicted at left) demonstrates severe left ventricular dilation in $VHL^{-/-}$ hearts. For $VHL^{+/+}$ and $VHL^{-/-}$ hearts, the image on the right is an enlargement of the short-axis image. The yellow lines depict relative intraventricular diameters during diastole. (C) Long-axis two-dimensional echocardiography (orientation depicted at left) demonstrating chamber dilation and the presence of a tumor in the left atrium. LV, left ventricle; RV, right ventricle; LA, left atrium; the yellow arrow depicts a tumor. (D) Echocardiographic analysis of cardiac function reveals significantly reduced fractional shortening during contraction of $VHL^{-/-}$ hearts and significant increases in both end-diastolic and end-systolic diameters of the left ventricle. Whereas these differences were significant at 5 months postbirth, these differences were not significant at 4 months, thus demonstrating the temporal progression of dysfunction and dilation. $n \geq 10$ mice per genotype. FS, fractional shortening; LVEDD, left ventricular end-diastolic diameter; LVESD, left ventricular end-systolic diameter; 4m and 5m, 4 and 5 months postbirth; ctrl, control littermates; KO, $VHL^{-/-}$. (E) Hemodynamic assessment reveals reduced rates of pressure increase and pressure decrease during left ventricular contraction in $VHL^{-/-}$ hearts ($+dP/dt$ and $-dP/dt$, respectively) and reduced peak developed pressures in $VHL^{-/-}$ hearts at baseline and during progressive infusion rates of dobutamine. Heart rates were similar in $VHL^{-/-}$ and $VHL^{+/+}$ (control littermate) hearts at all but the highest dose of dobutamine. (F) Heart weights and heart weight/body weight ratios were higher for the $cmVHL^{-/-}$ mice ($n \geq 12$ per genotype). (G) Cardiac deletion of VHL results in early and progressive mortality, beginning after 3 months postbirth. Concomitant deletion of VHL and HIF-1α in heart muscle prevents this increased mortality. dKO, double knockout. Curve generated with ≥20 mice per genotype.

RESULTS

Loss of VHL in cardiac muscle results in severe heart failure and early mortality; concomitant deletion of HIF-1α prevents this phenotype. To investigate the role of VHL in the heart and the effects of chronic myocardial activation of the HIF pathway, we generated mice with deletion of VHL specifically from cardiac myocytes ($cmVHL^{-/-}$ mice) by crossing MLC2v-Cre haploid knock-in mice with VHL loxP mice. $cmVHL^{-/-}$ mice were born at expected gene frequencies without embryonic or early postnatal lethality and with no evident early physical distress. At 3 months of age, heart function in the $cmVHL^{-/-}$ mice was not significantly different from that in wild-type littermates, but by 5 months severe cardiac dilation and heart failure were apparent, as were increases in cardiac weight and heart weight/body weight ratios (Fig. 1A to F). Further, intracardiac masses were apparent premortem by cardiac ultrasound examination in a subset of these mice (Fig. 1C). $cmVHL^{-/-}$ mice also exhibited early mortality (Fig. 1G). Given that the major known function of VHL is to reduce HIF levels under normoxic conditions, we hypothesized that the $cmVHL^{-/-}$ phenotype was at least partially HIF mediated and HIF dependent. To evaluate this, we generated mice with concomitant cardiospecific deletion of both VHL and HIF-1α (cmVHL/HIFdKO mice). cmVHL/HIFdKO mice were born at expected Mendelian frequency, were healthy, and exhibited none of the phenotypic features that developed progressively in the $cmVHL^{-/-}$ mice. Cardiac function in these mice was normal (not shown) and they had normal longevity (Fig. 1G), strongly confirming that HIF-1α plays a crucial role in the pathogenesis of the $cmVHL^{-/-}$ phenotype.

To understand the pathophysiological basis for the HIF-1α-dependent $cmVHL^{-/-}$ phenotype, we began with an examination of the histological and ultrastructural features of the $cmVHL^{-/-}$ hearts. Histologic examination of the myocardium revealed prominent myocyte degeneration and loss, replacement fibrosis, vacuolization, and lipid accumulation (Fig. 2A to I). Ultrastructural analysis revealed myofibrillar rarefaction, disarray, and disassembly (Fig. 2J to L). The structure of the myocyte nuclei was also markedly abnormal, with redundancy and loss of integrity of the nuclear envelope, nuclear blebs, and nuclear inclusions, as well as severe morphological changes reminiscent of nuclear laminopathies associated with cardiac dysfunction (Fig. 2M to P). Finally, there were mitochondrial inclusions and a marked increase in ultrastructural features of

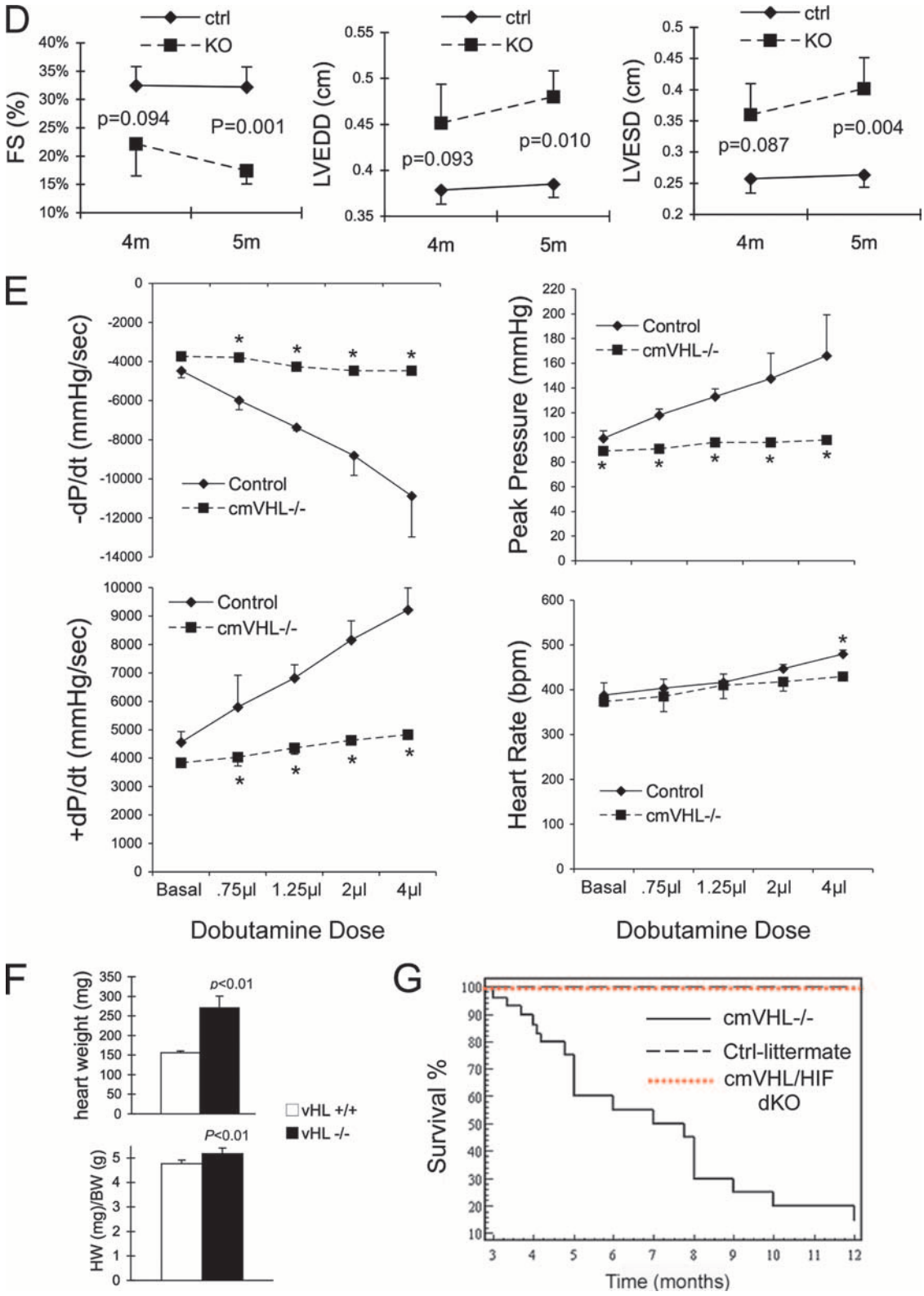

FIG. 1—*Continued*.

autophagy (Fig. 2K, Q, and R). These changes were apparent throughout the left ventricle, independent of the presence or absence of intracardiac masses. Many of these ultrastructural features have been described for human IHD and for dilated cardiomyopathy. To investigate whether the ultrastructural evidence of mitochondrial autophagy was correlated with a decrease in ventricular mitochondrial content, we performed quantitative PCR for mitochondrial DNA. These studies con-

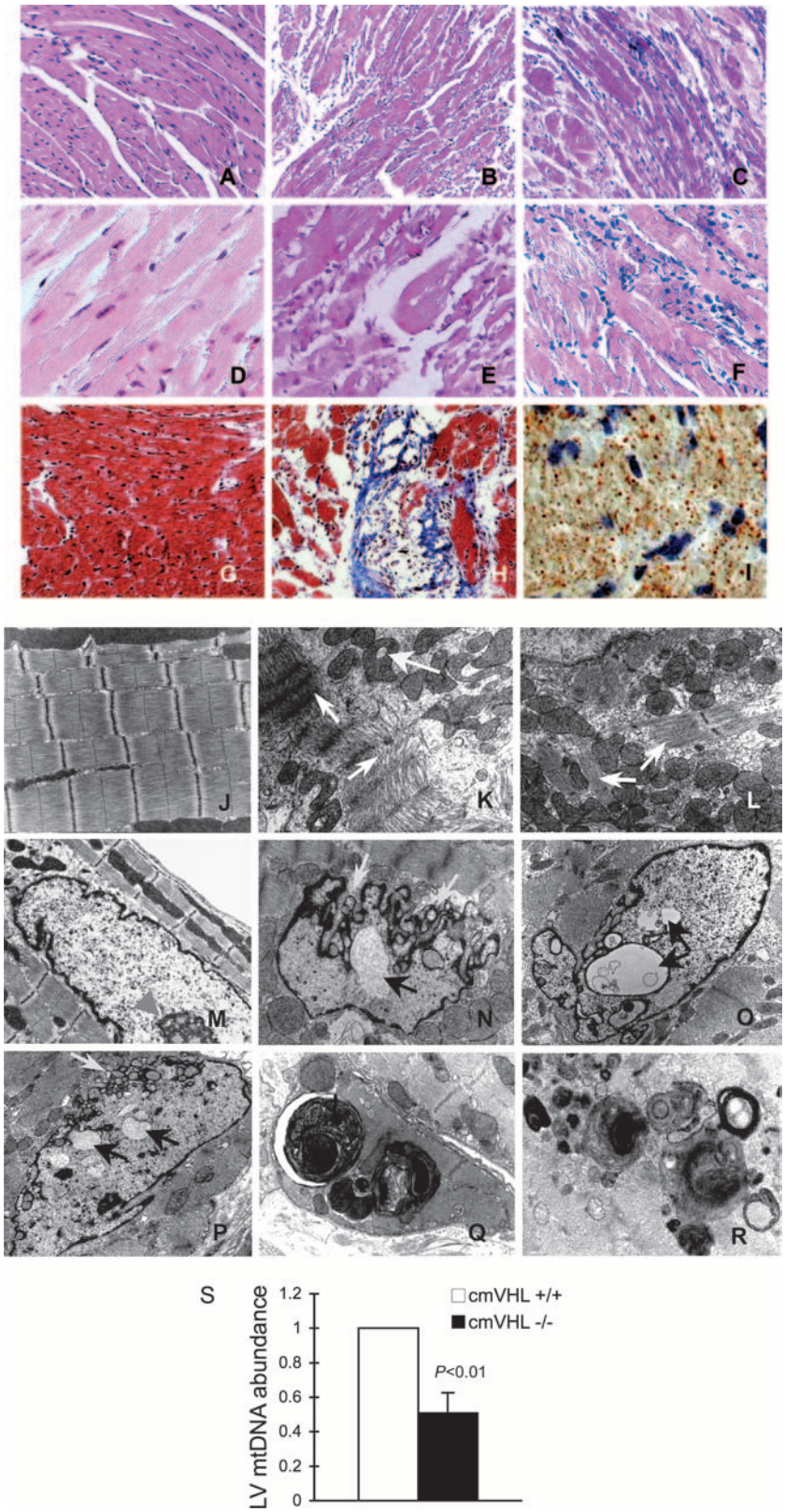

FIG. 2. Absence of VHL from cardiac myocytes results in myocyte disassembly and loss, replacement fibrosis, automacrophagocytosis, lipid accumulation, organelle inclusions, and an altered nuclear envelope. (A to C) Hematoxylin and eosin staining (200× magnification) of myocardia from mice with cardiac myocyte-specific deletion of VHL ($cmVHL^{-/-}$) reveals severe myocardial degeneration with thinning and loss of cardiac muscle bundles (B and C) compared to $VHL^{+/+}$ control littermate hearts (A). Also visible is patchy infiltration by inflammatory cells (C). (D to F) Analysis at 400× magnification further demonstrates myocardial degeneration and nonuniformity of cardiac muscle bundles (E and F) and

firmed a significant decrease in mitochondrial number for cmVHL$^{-/-}$ hearts (Fig. 2S).

cmVHL$^{-/-}$ mice develop malignant cardiac tumors, a HIF-1α-dependent phenotype. When examined directly, the intracardiac masses identified upon echocardiography (Fig. 2C) were found to be cardiac neoplasms (Fig. 3A to E). They occurred with a frequency of at least 45% of all cmVHL$^{-/-}$ mice (Fig. 3F) and never developed in wild-type littermates or cmVHL/HIFdKO mice. Tumors were found in the left ventricle, in the right ventricle growing from the intraventricular septum, and growing into the left atrium from the atrial-ventricular region (Fig. 3A to D). These intracardiac tumors were also capable of metastasis, indicative of their malignancy (Fig. 3E). Light microscopy revealed sheets of pleomorphic cells and loss of normal myocardial architecture (Fig. 3G to I). Further, intratumoral regions stained positive for desmin and exhibited striations consistent with the formation of myofibrils (Fig. 3J). The gross morphometric and histological features were not consistent with hemangioma formation. Metastatic tumors exhibited similar morphology and histology (Fig. 3K and L). Transformed cells were cultured from multiple successive tumors and evaluated for structural and functional features (Fig. 3M to U). These features included spindle cell and spider cell morphology (Fig. 3M and N), loss of contact growth inhibition (Fig. 3O), anchorage-independent growth in soft agarose (Fig. 3P), the ability to form myotubes and multinuclear cells in culture (Fig. 3Q and R), and positive staining for desmin (Fig. 3S and T), many of which are features observed for rhabdomyosarcoma. Immunostaining for PECAM was negative. Finally, these cells were fully capable of tumor formation when injected subcutaneously in immune-deficient (Rag2$^{-/-}$) mice (Fig. 3U) and could then be recultured from these tumors (data not shown). To date, each tumor cell line has remained viable and passageable over at least 100 passages. Quantitative RT-PCR analysis of VHL expression and genomic analysis of tumor tissue confirmed markedly decreased VHL expression and a high rate of VHL excision in these tumors (Fig. 3V and W).

cmVHL$^{-/-}$ hearts paradoxically exhibit nonuniform hypovascularity. One of the most prominent clinical findings for VHL syndrome is the development of hemangioblastomas, thought to be secondary to HIF-1α-mediated vascular endothelial growth factor (VEGF) expression in the absence of VHL. Accordingly, we expected that the loss of VHL in cardiac myocytes would lead to markedly increased coronary vascularity and perhaps to the development of cardiac hemangiomas. Interestingly, cmVHL$^{-/-}$ hearts actually exhibited decreased average capillary counts relative to littermate control hearts (Fig. 4A and B), possibly partially attributable to the myocyte loss and replacement fibrosis observed for these hearts. Despite this decrease in average capillary counts, total PECAM and Flt-1 protein levels were elevated in the cmVHL$^{-/-}$ hearts (Fig. 4C). To determine whether this might reflect an increase in larger-diameter vessels, we created and analyzed vascular casts of cmVHL$^{+/+}$ and cmVHL$^{-/-}$ hearts. At the macrovascular level, defined as those vessels capable of distinct resolution and visualization by stereoscopic analysis of coronary vascular casts, there was no evidence increased vascularity in the cmVHL$^{-/-}$ hearts. Conversely, there were areas of decreased vascularity in these hearts, although there was considerable variability from region to region within each cmVHL$^{-/-}$ heart (Fig. 4D and E). We hypothesized that the paradox between the PECAM and Flt-1 protein elevation and the hypovascularity we documented might be partially attributable to increased infiltration of the cmVHL$^{-/-}$ hearts by marrow-derived cells with these markers. Indeed, histological and immunohistological analysis revealed significant numbers of inflammatory cells within these hearts (data not shown).

Forced expression of HIF-1α in the heart by gene transfer induces lipid accumulation in the myocardium and failure to thrive. Although the VHL/HIF-1α double gene excision studies documented a crucial and deleterious role of HIF-1α in the genesis of the cmVHL$^{-/-}$ phenotype, we examined the direct effect of chronic HIF-1α expression in hearts in which the VHL gene was intact. To accomplish this, we injected the myocardium of day 1 neonatal mice with recombinant adenovirus encoding either wild-type HIF-1α, HIF-1α-VP16 (a stable chronically active HIF-1α), or beta-galactosidase (control). Injection of the mouse heart at this age diminishes adenovirus-induced immune responses and results in the expression of the transgene into adulthood. Cardiac gene transfer with either HIF construct induced marked retardation in the growth of the recipient mice (Fig. 5A and B) and an increase in heart weight/body weight ratios (Fig. 5C), as well as a trend toward increased heart absolute weights (data not shown). There was also a marked increase in cardiac lipid content as assessed by oil red O staining (Fig. 5E and F), recapitulating the finding for cmVHL$^{-/-}$ hearts. There were also, as expected, significant alterations in the expression of HIF-responsive genes in the HIF-injected hearts, and the level of induced expression correlated closely with the expression of the HIF-VP16 construct (Fig. 5G).

Deletion of VHL results in significantly increased HIF-1α binding activity, chronic activation of hypoxia-responsive genes, phosphorylation of the cMET and epidermal growth factor receptors (EGFR), and Ras activation in the heart. Although ubiquitylation by VHL is the major mechanism

cellular infiltration (F) compared to control myocardium (D). (G and H) Myocyte loss and replacement fibrosis is also shown by Mason's trichrome staining of cmVHL$^{-/-}$ hearts (H) versus control littermates (G). (I) cmVHL$^{-/-}$ hearts also accumulate lipids, as shown by oil red O staining. (J to L) Ultrastructural analysis by transmission EM demonstrates disarray and disassembly of myofibrils (white arrows), irregular spacing of Z-bands, irregular orientation of myofibrils, and mitochondrial inclusions (yellow arrow) in cmVHL$^{-/-}$ hearts (K and L) versus the normal architecture of control hearts (J). (N to P) Nuclei from cmVHL$^{-/-}$ hearts exhibit irregular nuclear morphology with prominent folding and blebbing of the nuclear envelope (blue arrows) and multiple nuclear inclusions (black arrows) compared to the normal nuclear architecture in control myocardium (M; arrowhead indicates nucleolus). (Q and R) Multilaminar vesicles (autophagosomes) containing whole organelles (e.g., mitochondria), myofibrils, and other cellular debris were seen frequently in cmVHL$^{-/-}$ hearts, indicating increased autophagy/macroautophagy. (S) Quantitative PCR for mitochondrial DNA revealed a decrease in cmVHL$^{-/-}$ hearts ($n = 5$ per genotype). For ultrastructural and histological analysis, ≥5 hearts per genotype were studied, with at least five sections and five separate fields/section evaluated per heart.

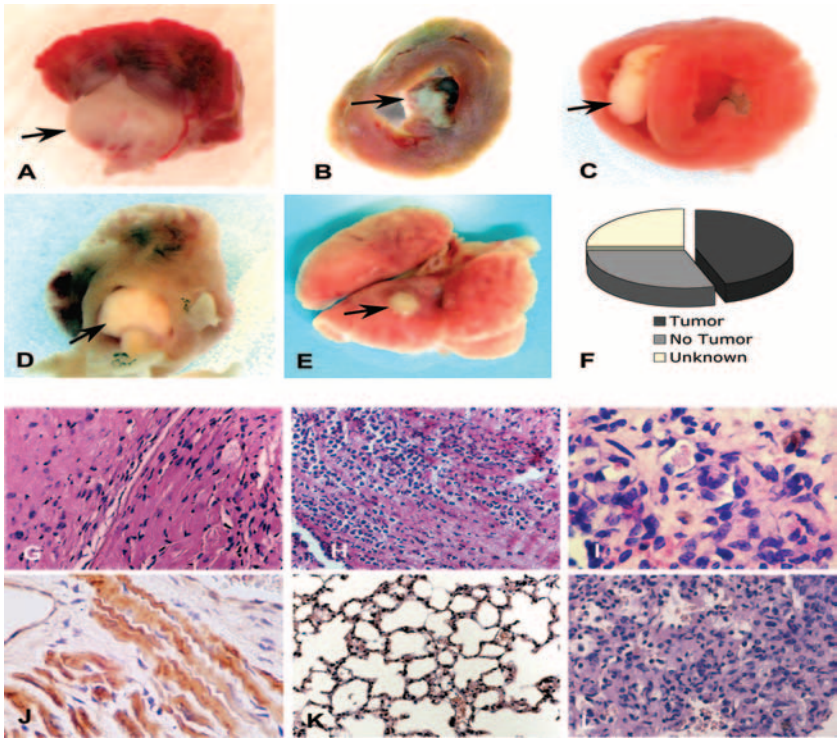

FIG. 3. Cardiac myocyte-specific deletion of VHL results in primary cardiac tumors in the heart that have the capacity to metastasize. (A to D) Spontaneous primary cardiac tumors growing from the atrial-ventricular junction into the left atrium (A and D), the intraventricular septum into the right ventricle (C), and the left ventricular free wall into the left ventricular chamber (D). Areas from which tumors develop are areas in which MLC2V-Cre is expressed and therefore where VHL is excised. (E) Metastatic tumor to lung. (F) Graphic representation of the incidence of tumors in cmVHL$^{-/-}$ mice. (G to I) Hematoxylin and eosin-stained sections of cmVHL$^{-/-}$ myocardium with tumor infiltration. At a magnification of ×200, the loss of myocardial normal myocardial architecture (J) (compare with Fig. 2A) and myocardial replacement by undifferentiated cells (G and H) are seen. (I) At a magnification of ×400, variable morphologies of nuclei and cells are seen. (J) Tumor tissue exhibits desmin staining and histological characteristics of myofibrillar structure, features consistent with rhabdomyosarcoma. (K) Normal lung histology from control littermate. (L) Histology of metastatic tumor in lung tissue. (M to U) Cultured tumor cells from cmVHL$^{-/-}$ hearts display multiple morphologies (M and N), lack contact inhibition (O), form colonies in soft agarose (P), and can form myotubes (Q). These cells can also become multinucleate and form myofibril-like structures (R), are desmin positive (S and T) (desmin staining is seen as green fluorescence), and form tumors in immunodeficient mice when injected subcutaneously (U) (arrow depicts tumor; $n = 4$). Quantitative RT-PCR (V) and quantitative PCR (W) of tumors revealed reduced VHL expression correlating with VHL gene excision.

whereby HIF-1α levels are suppressed, there are multiple additional levels of control of HIF activity. Therefore, it remained unclear that deletion of VHL in the heart would result in chronically elevated HIF-1α activity. We assessed this using a transcription factor ELISA to determine HIF-1α-specific HRE binding activity and found a greater-than-5.5-fold increase in nuclear extracts from cmVHL$^{-/-}$ hearts (Fig. 6A). There was no concomitant increase in HIF-1α mRNA, consistent with lost posttranslational destruction of HIF-1α in the absence of VHL as the predominant mechanism of increased HIF-1α activity (Fig. 6B). In conjunction with this increase in HIF-1α binding activity there were increased mRNA levels of multiple HIF-responsive genes (Fig. 6C). Among these were expected elevations in metabolism, angiogenesis, and matrix-associated genes, including the Glut-1, LDH-A, phosphoglycerate kinase, VEGF-A, PDGF-B, and TGF-β1 genes. There was also a more-than-21-fold increase in the expression of atrial natriuretic factor peptide, a marker of heart failure. Interestingly, fibronectin, assembly of which has been linked to VHL via a non-HIF pathway (44), was increased (4.1 ± 0.9)-fold ($P = 0.01$). Real-time PCR documented an ~90% VHL gene deletion in cardiac myocytes from cmVHL$^{-/-}$ mice and no detectable deletion in noncardiac cells, consistent with our previous experience generating conditional knockouts using MLC2v-Cre mice (13, 23).

To investigate potential mechanisms whereby cardiac dedifferentiation and malignant transformation might occur in the absence of VHL, we analyzed the activation of the Ras, TGF-α-EGFR, and cMET pathways. Forced expression of activated Ras in the heart has been shown to induce cardiac hypertrophy and dysfunction (24), the TGF-α-EGFR pathway has been implicated in the genesis of VHL-associated renal cell carcinoma, and cMET activation has been specifically implicated in the pathogenesis of rhabdomyosarcoma. Total and activated Ras protein levels were markedly elevated in cmVHL$^{-/-}$ hearts (Fig. 6D). TGF-α, a ligand for EGFR that has been implicated in tumorigenesis, was increased (4.5 ± 1)-fold at the mRNA level in cmVHL$^{-/-}$ hearts ($P < 0.05$), and EGFR was increased (1.61 ± 0.3)-fold ($P < 0.01$). This was accompanied by EGF-R phosphorylation, a marker of activation (Fig. 6C and D). cMET mRNA was increased (1.8 ± 0.3)-fold ($P < 0.01$) and was accompanied by

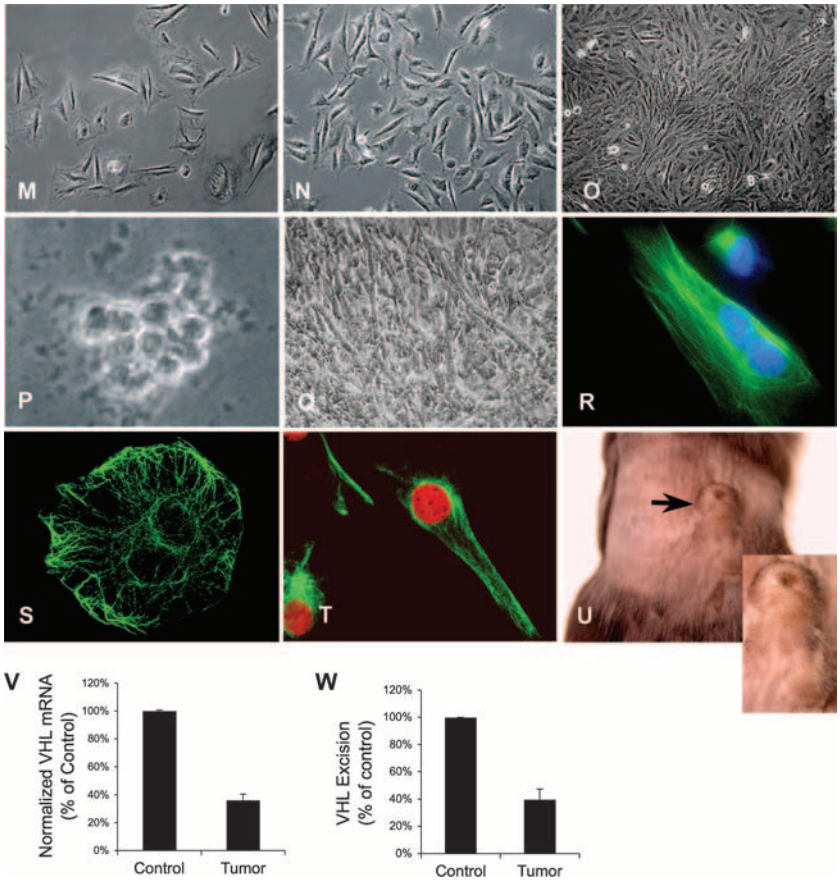

FIG. 3—*Continued*.

phosphorylation of this receptor, indicative of activation (Fig. 6C and D). Survivin, an apoptosis inhibitor that is upregulated in a variety of human malignancies including rhabdomyosarcoma and has been implicated as contributing to the pathogenesis of cancer, was increased by (3.1 ± 1)-fold ($P < 0.05$). Conversely, TSC1 and TSC2, associated with development of nonmalignant rhabdomyoma, were unchanged (data not shown). All of the above data were obtained from the left ventricular tissue of hearts devoid of observable tumor.

DISCUSSION

Here we show that the loss of VHL in heart muscle results in the chronic activation of the HIF-1α hypoxia response pathway, progressive cardiac degeneration, severe heart failure, malignant transformation, and death. That these changes do not occur when HIF-1α and VHL are concomitantly deleted strongly implicates HIF-1α in the genesis of these pathologies. These data document for the first time a crucial role for VHL in the heart and also strongly support a conclusion that chronic activation of the HIF pathway, such as occurs in advanced IHD (36), is a two-edged sword that plays an important role in the pathogenesis of progressive cardiac dysfunction. The clinical implications of this conclusion are significant, suggesting that modifications of the hypoxia response could prevent progressive cardiac dysfunction in various clinical settings, that recurrent ischemia might lead to progressive cardiac dysfunction independent of myocardial infarction, and that recurrent ischemia perhaps should thus be more determinedly avoided. More broadly, these findings raise the question of whether adaptive hypoxia responses play a pathophysiological role in other clinical settings in which recurrent ischemia or hypoxia are encountered, such as sleep apnea and cerebrovascular dementia.

Others and we have documented several crucial basal and adaptive functions of HIF-1α in the heart (7, 23, 29). It would thus seem inconsistent to concomitantly implicate HIF in the pathophysiology of cardiac disease. We contend that this seeming paradox is a function of the chronicity and intensity of HIF pathway activation. Short-term elevation of HIF levels in response to hypoxia or ischemia drive beneficial adaptive processes such as angiogenesis and appropriate shifts in cell metabolism. Accordingly, promoting a short-term increase in HIF-1α levels may prove clinically beneficial; this approach is currently being evaluated in patients with IHD and in patients with peripheral arterial disease (15, 48). Preliminary reports from these trials have indicated that short-term adenovirus-mediated expression of HIF-1α is safe (15, 48, 60). In our current study, cmVHL$^{-/-}$ mice do well for the first 3 months of life despite elevated HIF levels. This is consistent with our contention that the chronicity of HIF pathway activation is a major determinant of whether HIF responses are adaptive or pathological.

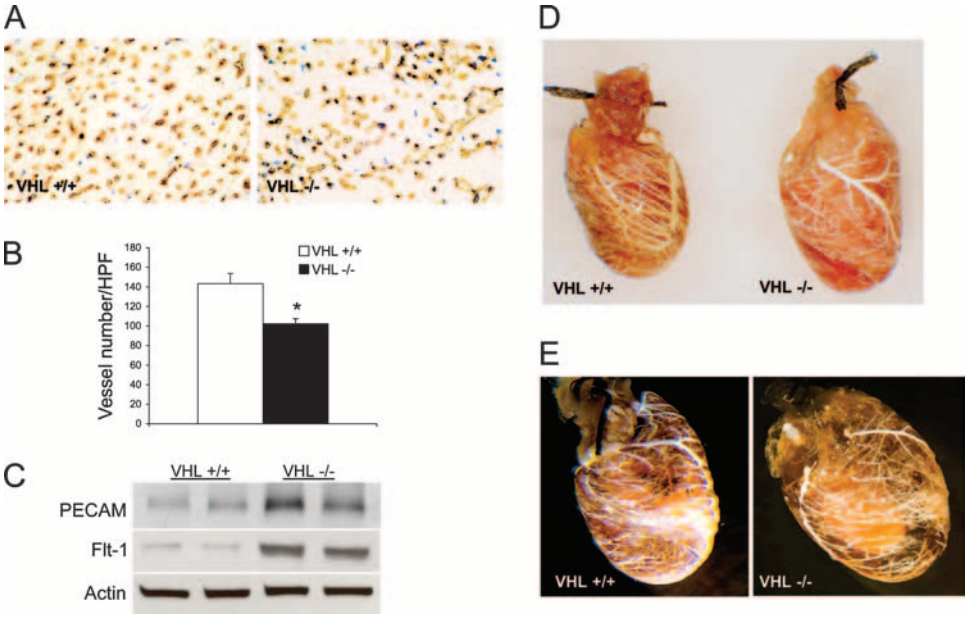

FIG. 4. cmVHL$^{-/-}$ hearts exhibit nonuniform hypovascularity. (A and B) Anti-PECAM immunostaining reveals a significant decrease in average capillary counts in cmVHL$^{-/-}$ hearts. (C) Despite decreased average capillary counts, there was an increase in total PECAM and Flt-1 protein in cmVHL$^{-/-}$ hearts, possibly attributed to myocardial infiltration by PECAM/Flt-1-positive inflammatory cells (Fig. 2C and F). (D and E) Casts of the coronary vasculature demonstrate regional variability and decreased macrovascular density in cmVHL$^{-/-}$ hearts. *, $n \geq 5$ hearts per genotype for vessel counts; $n = 4$ hearts per genotype for casts.

Many of the pathological features observed for cmVHL$^{-/-}$ hearts are seen for human hearts with advanced IHD, hibernating myocardium, and various cardiomyopathies (9–11, 53). The precise mechanisms mediating all these pathological changes in cmVHL$^{-/-}$ hearts remain unclear. We demonstrate here that they are, however, HIF-1α dependent, and several potential HIF-associated mechanisms are identifiable. We demonstrate marked lipid accumulation in cmVHL$^{-/-}$ hearts and in hearts chronically expressing an activated/stable HIF-1α, supporting an important role of HIF-1α in mediating this phenotype. This is important, as lipid accumulation in the myocardium has been documented in human cardiomyopathy, and lipotoxicity has been put forth as an important mechanism of progressive cardiac dysfunction and myocyte loss (53). HIF is intrinsically involved in the regulation of an array of metabolism-related genes encoding proteins that could contribute to lipid accumulation and lipotoxicity in the heart. Examples include the glucose transporter Glut1, the glycolytic enzymes, and ANGPTL4 (angiopoietin-like 4), a protein that has significant effects on lipid metabolism and alters lipoprotein lipase activity. The HIF pathway has also been implicated in cross talk with the AMP kinase pathway and may have effects on mitochondrial energetics, all of which could contribute to altered lipid metabolism.

The prevalence of organelles and myofibrils within double-membrane vesicles seen on ultrastructural analysis of cmVHL$^{-/-}$ hearts is consistent with increased myocardial autophagy (55, 64), and the reduction in mitochondria we document for these hearts is consistent with loss via autophagy. Autophagy has been linked to abnormal lipid metabolism, and this represents one potential mechanism for our findings. Another potential link is BNIP3, a member of the bcl2/adenovirus E1B-interacting protein family that has been implicated in regulating autophagy (59). BNIP3 is encoded by a HIF-regulated gene, and BNIP3 levels were highly induced in cmVHL$^{-/-}$ and HIF-encoding-adenovirus-transduced hearts. Another consideration is that autophagy can be induced in settings in which cells are "starving" and use self-digestion to provide nutrients and building blocks to maintain cell viability. The mTOR (*m*ammalian *t*arget of *r*apamycin) pathway functions in part to coordinate cellular events with nutrient availability and has been linked to the regulation of cellular autophagy (61). Multiple studies have documented cross talk between the mTOR and HIF pathways (35), but whether HIF and mTOR cooperate in the regulation of autophagy is unknown. It is interesting, however, to consider that activation of the HIF pathway promotes a cellular state in which "starvation" occurs in the setting of nutrient abundance, possibly via uncoupling oxidative phosphorylation and shunting of metabolism to lower-energy pathways such as glycolysis. Multiple features shared by cmVHL$^{-/-}$ hearts and chronically ischemic human myocardium, including myofibrillar rarefaction, are, like autophagy, processes consistent with a cellular response to either decreased nutrient/energy availability or an inability to functionally utilize available nutrients. Rarefaction also occurs in neurons of patients with cerebrovascular dementia, and autophagy has been recently shown to be a prominent neuropathological component of dementia (43, 63). Although clearly beyond the objective findings of our current study, it is compelling to consider that noninfarct degeneration in IHD and cerebrovascular disease may share a mechanistic link involving chronic activation of the HIF pathway.

The development of HIF-1α gene therapy for IHD and peripheral arterial disease is largely tied to the role of HIF in mediating proangiogenic responses to tissue hypoxia. The vas-

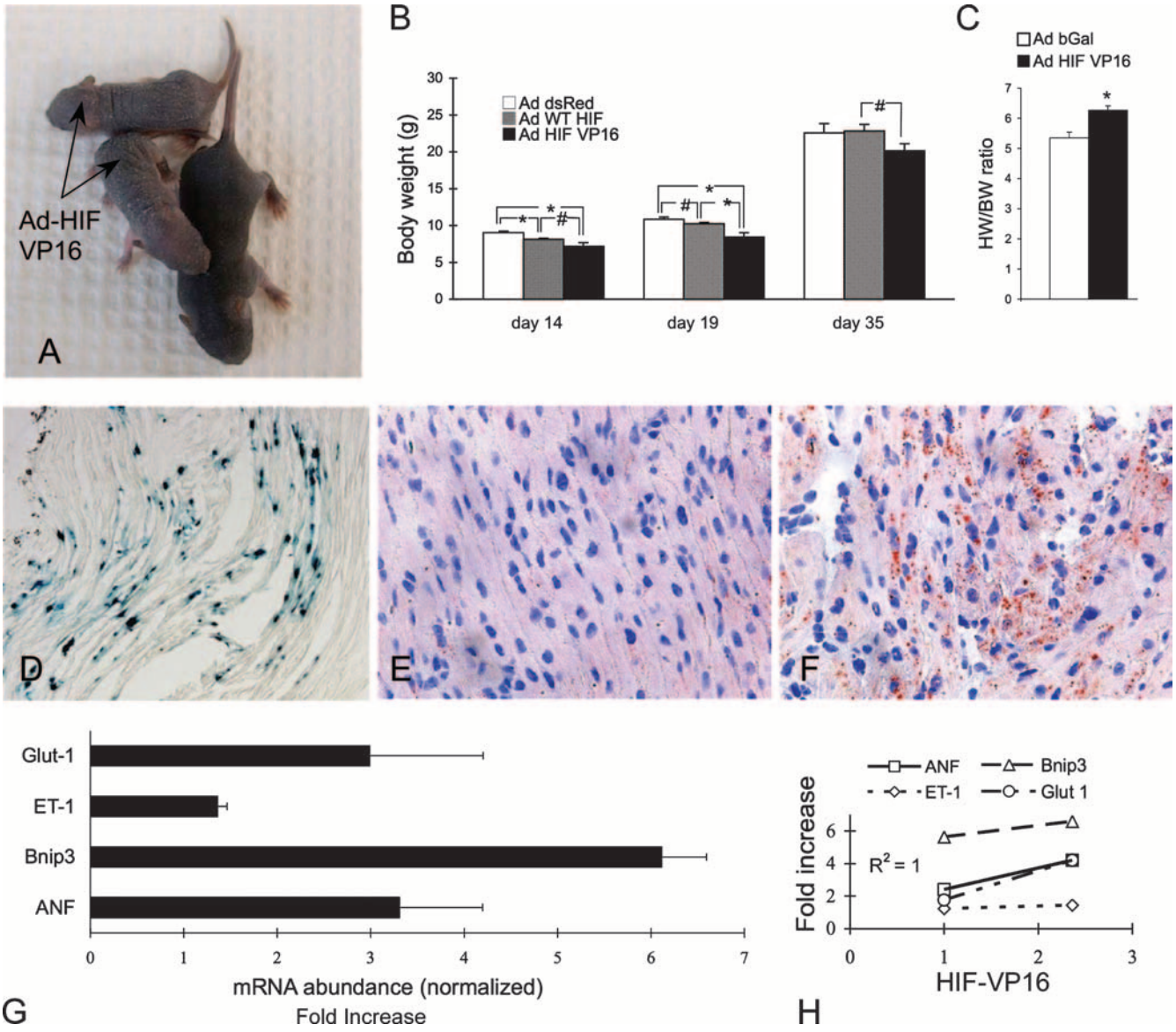

FIG. 5. Forced cardiac overexpression of HIF-1α results in myocardial lipid accumulation and failure to thrive. On day 1 postbirth, adenovirus encoding either beta-galactosidase (Ad-β-Gal [Ad bGal]) or a stable form of HIF-1α (Ad-HIFVP16) was delivered to the hearts of neonatal mice. (A to C) Neonatal expression of Ad-HIFVP16 in the heart resulted in significant growth retardation and increased heart weight/body weight ratios 10 days postbirth (#, $P = 0.07$; ∗, $P < 0.05$). WT, wild type. (D) Illustration of the general efficiency of gene delivery to the heart 10 days after neonatal Ad-β-Gal gene delivery. (E and F) Oil red O staining reveals a marked increase in myocardial lipid content in Ad-HIFVP16 hearts (F) versus those that received Ad-β-Gal (E). (G) Ad-HIFVP16 expression in the neonatal heart results in marked induction of HIF-responsive genes (assessment by real-time RT-PCR; values relative to those for Ad-β-Gal hearts and normalized to 18S; onefold is baseline expression). (H) Induction of gene expression correlates with the efficiency of gene delivery as defined by HIF-VP16 expression in the heart (basal VP16 value, 0; VP16 of 1 was the lowest level detected). ANF, atrial natriuretic factor; ET-1, endothelin 1; Bnip3, bcl2/adenovirus E1B-interacting protein 3; Glut-1, glucose transporter 1. $n \geq 5$ per group.

cular abnormalities seen for von Hippel-Lindau syndrome are in fact attributable to HIF-mediated angiogenesis, and HIF is thought to play an important role in the vascularization of tumors. Paradoxically, cmVHL$^{-/-}$ hearts exhibit regional hypovascularity at both microvessel and macrovessel levels. One possible explanation involves the myocyte loss and replacement fibrosis seen for cmVHL$^{-/-}$ hearts. Fibrotic regions tend to be less vascular than normal myocardium. Further, cardiac myocytes are the major source of some crucial angiogenic factors in the heart, such as VEGF, and the loss of myocytes thus decreases the regional production of these angiogenic factors (16). Another important consideration is that the HIF pathway regulates the expression of both pro- and antiangiogenic factors, and thus the relationship between HIF and angiogenesis is more complex than that between VEGF and angiogenesis, for example. Illustrative of this are data we generated from mice with cardiac myocyte- and endothelium-specific deletions of VEGF and HIF-1α (16, 23, 57). Cardiac

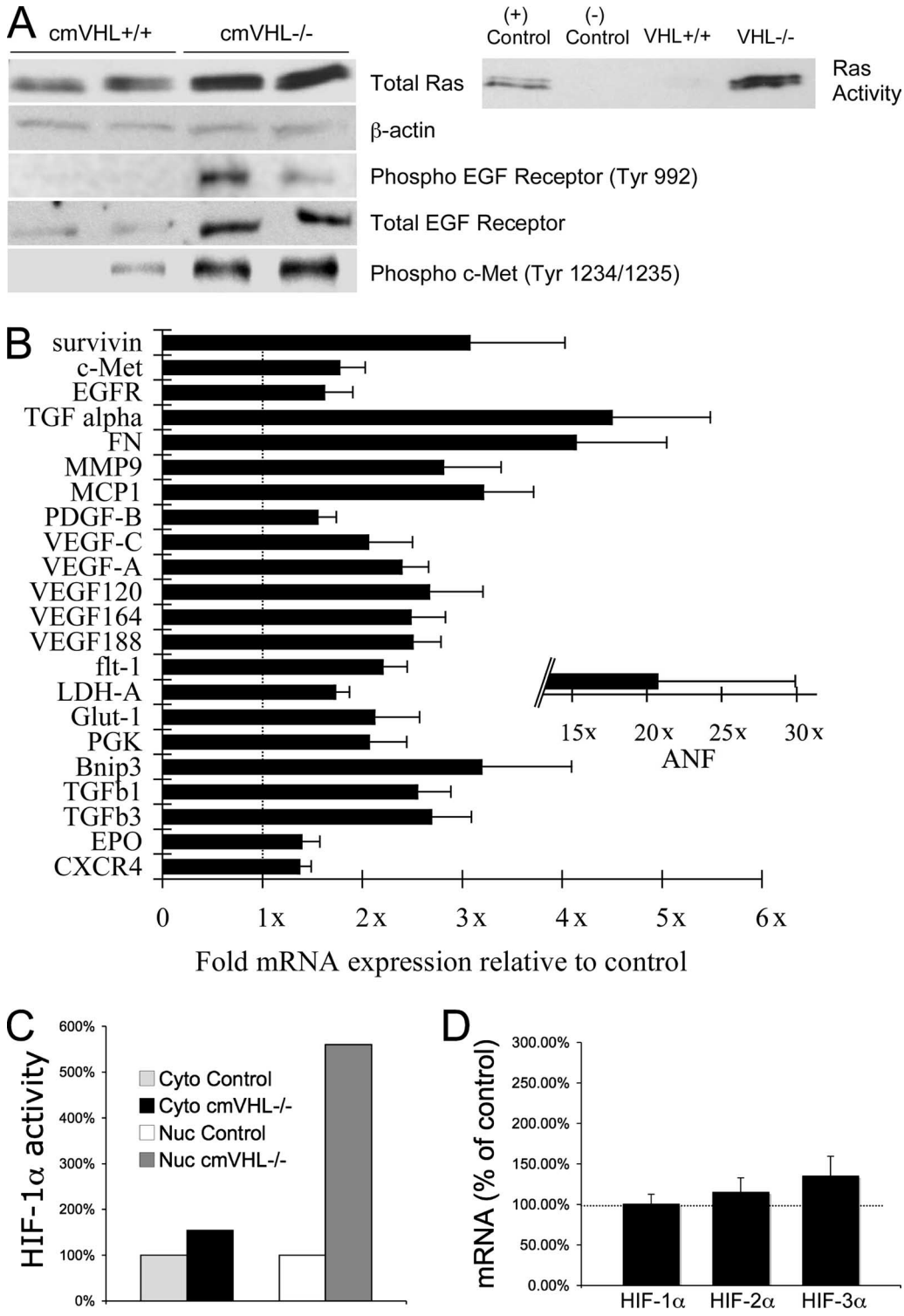

FIG. 6. VHL deletion in cardiac myocytes is associated with Ras activation, EGFR and cMET phosphorylation, altered expression of HIF-responsive genes, and increased HIF-1α HRE binding activity. (A) cmVHL$^{-/-}$ hearts have higher total and activated Ras levels and higher levels of phosphorylated (active) cMET and EGFR. (B) Real-time RT-PCR revealed significant alterations in the expression of a variety of HIF-responsive genes (normalized for 18S; "1x" indicates identical expression with control littermates). FN, fibronectin; MMP9, metalloproteinase 9 (gelatinase); MCP-1, monocyte chemotactic protein 1; PDGF, platelet-derived growth factor B; PGK, phosphoglycerate kinase; Glut1, glucose transporter 1; Bnip3, bcl2/adenovirus E1B-interacting protein; EPO, erythropoietin. (C) Pooled nuclear extracts from cmVHL$^{-/-}$ hearts demonstrate higher HIF-1-specific HRE binding (HIF-1α transcription factor binding ELISA). Cyto, cytoplasmic extract; Nuc, nuclear extract. (D) Real-time RT-PCR reveals no significant alterations in mRNA levels for HIF-1 to -3α in cmVHL$^{-/-}$ hearts, consistent with VHL posttranslational control of HIF protein levels (mRNA abundance in control littermate hearts depicted as 100% [dotted line]). $n \geq 5$ hearts per genotype.

deletion of HIF-1α resulted in only a mild reduction of vascularity, whereas cardiac deletion of VEGF resulted in a more pronounced hypovascularity and in variable levels of embryonic lethality. Endothelial deletion of HIF-1α resulted in no significant basal decrease in vascularity. Thus, although HIF-1α is intrinsically involved in linking hypoxia to an angiogenic response, the relationship appears to be more complex than initially thought.

One of the most surprising findings of this study is the development of malignant cardiac tumors. Deletion of VHL in other tissues in mice has resulted in hemangiomas but not malignant transformation (22, 30, 39, 40, 46). Further, the myocardium is among the most tumor-resistant mammalian tissues. That mice with concomitant deletion of VHL and HIF do not manifest malignant transformation of the heart establishes that this occurrence is HIF-1α dependent, although clearly other VHL-dependent HIF-1α-independent functions may be involved. Elevated HIF levels and expression of HIF-responsive genes have been shown for a myriad of human malignancies, but it has remained unclear whether HIF pathway activation contributes to the transformation process or is only secondarily involved in the vascularization and metabolic switching of ischemic neoplasms. Recently it was shown that hypoxia-independent overexpression of HIF-1α precedes the development of hepatic malignancies in mice, suggesting but not proving HIF involvement in early carcinogenesis (56). In another study, knockdown of HIF-2α by a small interfering RNA approach prevented VHL-deficient renal cell carcinoma cells from efficiently forming tumors in mice (32). This again shows that the HIF pathway is involved in tumor growth but does not establish a role in malignant transformation.

If the HIF pathway is indeed involved in the transformation process, how might this occur? The cardiac tumors in cmVHL$^{-/-}$ mice exhibit features consistent with rhabdomyosarcoma. Constitutive expression of hepatocyte growth factor in mice, when combined with the loss of the cell cycle control protein p16 (INK4a), is associated with highly penetrant occurrence of rhabdomyosarcoma in skeletal muscle (54). The receptor for hepatocyte growth factor is cMET, which is a HIF-responsive gene (45). cMET mRNA is elevated in cmVHL$^{-/-}$ hearts, as is the active phosphorylated form of this receptor, thus providing a link between HIF-1α and at least one pathway associated with malignancy in muscle. Another link is TGF-α, which has been shown to be VHL responsive via both HIF-dependent and -independent pathways (21, 31). TGF-α and its receptor, EGFR, are both expressed at higher levels in cmVHL$^{-/-}$ hearts, and the active phosphorylated form of EGFR is also increased. TGF-α-EGFR signaling, as an autocrine loop, has been implicated in the genesis of renal cell carcinoma in human VHL syndrome (8, 21, 31). EGFR activation has also been implicated in cardiac hypertrophy and cardiomyocyte proliferation and has been shown to play an important role in cardiac development (2, 19, 58). Survivin, a protein that is elevated in a wide array of malignancies and linked to the pathophysiology of tumor progression (1), was also markedly induced in cmVHL$^{-/-}$ hearts.

Another mechanistic consideration relates to the abnormal nuclear morphology exhibited in cmVHL$^{-/-}$ hearts. These changes resemble nuclear morphology in human laminopathies, including the aging syndrome Hutchinson-Gilford progeria, Emery-Dreifuss muscular dystrophy, and lamin A/C-related cardiomyopathies (4). These syndromes are caused by abnormalities in genes encoding proteins that define the nuclear architecture and envelope integrity, including lamins A, B, and A/C. Recently, it was shown that primary fibroblasts from patients with laminopathy display altered genomic organization and a higher propensity to undergo apoptosis. Further, the incidence of malignancy in patients with laminopathy appears to be elevated, and methylation of the lamin A gene is associated with human leukemia and lymphoma. This raises the question of whether a HIF- or VHL-associated alteration in nuclear architecture could lead to altered genomic organization or other epigenetic changes that could promote cell loss or even transformation. The answer to this question is beyond the scope of the current study, but it is interesting that nuclear abnormalities have been described for failing or ischemic human heart muscle and that skeletal myopathy and cardiomyopathy are prominent features of various laminopathies.

We show that the concomitant deletion of HIF-1α and VHL is sufficient to prevent the tumorigenesis observed for cmVHL$^{-/-}$ mice, thus establishing that the cmVHL$^{-/-}$ phenotype is HIF-1α dependent. This does not, however, preclude the contribution of a lost HIF-independent VHL function or the involvement of HIF-2α and/or HIF-3α, which are also regulated by VHL. The repertoires of genes regulated preferentially by HIF-2α versus HIF-1α appear to be distinct, despite the ability of each to bind the same HRE (49). Thus, in the heart, the finding that concomitant deletion of VHL and HIF-1α abrogated the cmVHL$^{-/-}$ phenotype despite the continued presence of HIF-2α may be indicative of the nonredundancy of these two HIFs in cardiac muscle. Interestingly, a HIF-1α-expressing transgenic mouse has been reported, and it does not have the same phenotype as our cmVHL$^{-/-}$ mice (29). There are several potential explanations for this, including the requirement for concomitant contributions of HIF-2α or the loss of an additional VHL function. Most likely, however, is that simple transgenic overexpression of wild-type HIF-1α, as was done in that study, is not sufficient to overcome the normal VHL-dependent posttranslational degradation that naturally suppresses HIF levels during normoxia. Indeed, the aforementioned transgenic mice do not demonstrate increased HIF-1α protein levels in normoxic myocardium, although HIF-1α mRNA is increased. These mice do demonstrate increases in HIF-1α abundance above wild-type levels in response to induced ischemia and infarction, consistent with stabilization of HIF against posttranslational degradation during hypoxia.

Although our phenotype is definitively HIF-1α dependent, it clearly is possible that the loss of VHL causes HIF-independent events that are also essential to the development of the phenotype. While the best-characterized function of VHL is as the E3 ubiquitin ligase responsible for posttranslational reduction of HIF-1α, -2α, and -3α levels during normoxia (25–27, 37, 47, 50, 62), VHL does have additional documented functions and may have additional functions as yet unknown. VHL has been purported to play HIF-independent roles in regulating the fibronectin, cyclin D1, and RNA polymerase II genes and a variety of other genes that could contribute to the pathobiology of VHL-deficient clinical syndrome (3, 28). Irrespective of whether or not the cmVHL$^{-/-}$ cardiac phenotype involves HIF-independent as well as HIF-dependent VHL functions,

the fact that a single gene deletion in the most mitotically quiescent mammalian cell type could result in malignant transformation is intriguing, and further study may provide unique insights into the biology of malignant transformation. As the biology of VHL becomes better understood, the identity of additional VHL-associated pathways relevant to cardiovascular biology may be uncovered. At present, however, our findings strongly support two conclusions: VHL is required for maintenance of cardiac structure and function, and regulation of HIF-1α is central to this role of VHL.

ACKNOWLEDGMENTS

We thank William C. Sessa, Jordan S. Pober, and Tracy L. Bale for helpful comments and suggestions on the work and manuscript.

Work was funded by HL6401 and HL63770, both to F.J.G.

REFERENCES

1. **Altieri, D. C.** 2008. Survivin, cancer networks and pathway-directed drug discovery. Nat. Rev. **8:**61–70.
2. **Armstrong, M. T., D. Y. Lee, and P. B. Armstrong.** 2000. Regulation of proliferation of the fetal myocardium. Dev. Dyn. **219:**226–236.
3. **Bishop, T., K. W. Lau, A. C. Epstein, S. K. Kim, M. Jiang, D. O'Rourke, C. W. Pugh, J. M. Gleadle, M. S. Taylor, J. Hodgkin, and P. J. Ratcliffe.** 2004. Genetic analysis of pathways regulated by the von Hippel-Lindau tumor suppressor in Caenorhabditis elegans. PLoS Biol. **2:**e289.
4. **Burke, B., and C. L. Stewart.** 2002. Life at the edge: the nuclear envelope and human disease. Nat. Rev. **3:**575–585.
5. **Chen, J., S. W. Kubalak, and K. R. Chien.** 1998. Ventricular muscle-restricted targeting of the RXRalpha gene reveals a non-cell-autonomous requirement in cardiac chamber morphogenesis. Development (Cambridge) **125:**1943–1949.
6. **Christensen, G., S. Minamisawa, P. J. Gruber, Y. Wang, and K. R. Chien.** 2000. High-efficiency, long-term cardiac expression of foreign genes in living mouse embryos and neonates. Circulation **101:**178–184.
7. **Date, T., S. Mochizuki, A. J. Belanger, M. Yamakawa, Z. Luo, K. A. Vincent, S. H. Cheng, R. J. Gregory, and C. Jiang.** 2005. Expression of constitutively stable hybrid hypoxia-inducible factor-1alpha protects cultured rat cardiomyocytes against simulated ischemia-reperfusion injury. Am. J. Physiol. Cell Physiol. **288:**C314–C320.
8. **de Paulsen, N., A. Brychzy, M. C. Fournier, R. D. Klausner, J. R. Gnarra, A. Pause, and S. Lee.** 2001. Role of transforming growth factor-alpha in von Hippel–Lindau (VHL)(−/−) clear cell renal carcinoma cell proliferation: a possible mechanism coupling VHL tumor suppressor inactivation and tumorigenesis. Proc. Natl. Acad. Sci. USA **98:**1387–1392.
9. **Dispersyn, G. D., E. Geuens, L. Ver Donck, F. C. Ramaekers, and M. Borgers.** 2001. Adult rabbit cardiomyocytes undergo hibernation-like dedifferentiation when co-cultured with cardiac fibroblasts. Cardiovasc. Res. **51:**230–240.
10. **Elsasser, A., A. M. Vogt, H. Nef, S. Kostin, H. Mollmann, W. Skwara, C. Bode, C. Hamm, and J. Schaper.** 2004. Human hibernating myocardium is jeopardized by apoptotic and autophagic cell death. J. Am. Coll. Cardiol. **43:**2191–2199.
11. **Frangogiannis, N. G.** 2003. The pathological basis of myocardial hibernation. Histol. Histopathol. **18:**647–655.
12. **Giordano, F. J.** 2007. Therapeutic gene regulation: targeting transcription. Circulation **115:**1180–1183.
13. **Giordano, F. J.** 2001. A cardiac myocyte vascular endothelial growth factor paracrine pathway is required to maintain cardiac function. Proc. Natl. Acad. Sci. USA. **98:**5780–5785.
14. **Giordano, F. J.** 2005. Oxygen, oxidative stress, hypoxia, and heart failure. J. Clin. Investig. **115:**500–508.
15. **Giordano, F. J.** 2007. Therapeutic gene regulation: targeting transcription. Circulation **115:**1180–1183.
16. **Giordano, F. J., H. P. Gerber, S. P. Williams, N. VanBruggen, S. Bunting, P. Ruiz-Lozano, Y. Gu, A. K. Nath, Y. Huang, R. Hickey, N. Dalton, K. L. Peterson, J. Ross, Jr., K. R. Chien, and N. Ferrara.** 2001. A cardiac myocyte vascular endothelial growth factor paracrine pathway is required to maintain cardiac function. Proc. Natl. Acad. Sci. USA **98:**5780–5785.
17. **Giordano, F. J., and R. S. Johnson.** 2001. Angiogenesis: the role of the microenvironment in flipping the switch. Curr. Opin. Genet. Dev. **11:**35–40.
18. **Giordano, F. J., P. Ping, M. D. McKirnan, S. Nozaki, A. N. DeMaria, W. H. Dillmann, O. Mathieu-Costello, and H. K. Hammond.** 1996. Intracoronary gene transfer of fibroblast growth factor-5 increases blood flow and contractile function in an ischemic region of the heart. Nat. Med. **2:**534–539.
19. **Goishi, K., P. Lee, A. J. Davidson, E. Nishi, L. I. Zon, and M. Klagsbrun.** 2003. Inhibition of zebrafish epidermal growth factor receptor activity results in cardiovascular defects. Mech. Dev. **120:**811–822.
20. **Grunstein, J., J. J. Masbad, R. Hickey, F. Giordano, and R. S. Johnson.** 2000. Isoforms of vascular endothelial growth factor act in a coordinate fashion to recruit and expand tumor vasculature. Mol. Cell. Biol. **20:**7282–7291.
21. **Gunaratnam, L., M. Morley, A. Franovic, N. de Paulsen, K. Mekhail, D. A. Parolin, E. Nakamura, I. A. Lorimer, and S. Lee.** 2003. Hypoxia inducible factor activates the transforming growth factor-alpha/epidermal growth factor receptor growth stimulatory pathway in VHL(−/−) renal cell carcinoma cells. J. Biol. Chem. **278:**44966–44974.
22. **Haase, V. H., J. N. Glickman, M. Socolovsky, and R. Jaenisch.** 2001. Vascular tumors in livers with targeted inactivation of the von Hippel-Lindau tumor suppressor. Proc. Natl. Acad. Sci. USA **98:**1583–1588.
23. **Huang, Y., R. P. Hickey, J. L. Yeh, D. Liu, A. Dadak, L. H. Young, R. S. Johnson, and F. J. Giordano.** 2004. Cardiac myocyte-specific HIF-1alpha deletion alters vascularization, energy availability, calcium flux, and contractility in the normoxic heart. FASEB J. **18:**1138–1140.
24. **Hunter, J. J., N. Tanaka, H. A. Rockman, J. Ross, Jr., and K. R. Chien.** 1995. Ventricular expression of a MLC-2v-ras fusion gene induces cardiac hypertrophy and selective diastolic dysfunction in transgenic mice. J. Biol. Chem. **270:**23173–23178.
25. **Ivan, M., K. Kondo, H. Yang, W. Kim, J. Valiando, M. Ohh, A. Salic, J. M. Asara, W. S. Lane, and W. G. Kaelin, Jr.** 2001. HIFalpha targeted for VHL-mediated destruction by proline hydroxylation: implications for O2 sensing. Science **292:**464–468.
26. **Jaakkola, P., D. R. Mole, Y. M. Tian, M. I. Wilson, J. Gielbert, S. J. Gaskell, A. Kriegsheim, H. F. Hebestreit, M. Mukherji, C. J. Schofield, P. H. Maxwell, C. W. Pugh, and P. J. Ratcliffe.** 2001. Targeting of HIF-alpha to the von Hippel-Lindau ubiquitylation complex by O2-regulated prolyl hydroxylation. Science **292:**468–472.
27. **Kaelin, W. G., Jr.** 2002. Molecular basis of the VHL hereditary cancer syndrome. Nat. Rev. Cancer **2:**673–682.
28. **Kaelin, W. G., Jr.** 2007. The von Hippel-Lindau tumor suppressor protein: an update. Methods Enzymol. **435:**371–383.
29. **Kido, M., L. Du, C. C. Sullivan, X. Li, R. Deutsch, S. W. Jamieson, and P. A. Thistlethwaite.** 2005. Hypoxia-inducible factor 1-alpha reduces infarction and attenuates progression of cardiac dysfunction after myocardial infarction in the mouse. J. Am. Coll. Cardiol. **46:**2116–2124.
30. **Kleymenova, E., J. I. Everitt, L. Pluta, M. Portis, J. R. Gnarra, and C. L. Walker.** 2004. Susceptibility to vascular neoplasms but no increased susceptibility to renal carcinogenesis in Vhl knockout mice. Carcinogenesis **25:**309–315.
31. **Knebelmann, B., S. Ananth, H. T. Cohen, and V. P. Sukhatme.** 1998. Transforming growth factor alpha is a target for the von Hippel-Lindau tumor suppressor. Cancer Res. **58:**226–231.
32. **Kondo, K., W. Y. Kim, M. Lechpammer, and W. G. Kaelin, Jr.** 2003. Inhibition of HIF2alpha is sufficient to suppress pVHL-defective tumor growth. PLoS Biol. **1:**E83.
33. **Kondo, K., M. Yao, M. Yoshida, T. Kishida, T. Shuin, T. Miura, M. Moriyama, K. Kobayashi, N. Sakai, S. Kaneko, S. Kawakami, M. Baba, N. Nakaigawa, Y. Nagashima, Y. Nakatani, and M. Hosaka.** 2002. Comprehensive mutational analysis of the VHL gene in sporadic renal cell carcinoma: relationship to clinicopathological parameters. Genes Chromosomes Cancer **34:**58–68.
34. **Kuroki, T., F. Trapasso, S. Yendamuri, A. Matsuyama, H. Alder, M. Mori, and C. M. Croce.** 2003. Allele loss and promoter hypermethylation of VHL, RAR-beta, RASSF1A, and FHIT tumor suppressor genes on chromosome 3p in esophageal squamous cell carcinoma. Cancer Res. **63:**3724–3728.
35. **Land, S. C., and A. R. Tee.** 2007. Hypoxia-inducible factor 1alpha is regulated by the mammalian target of rapamycin (mTOR) via an mTOR signaling motif. J. Biol. Chem. **282:**20534–20543.
36. **Lee, S. H., P. L. Wolf, R. Escudero, R. Deutsch, S. W. Jamieson, and P. A. Thistlethwaite.** 2000. Early expression of angiogenesis factors in acute myocardial ischemia and infarction. N. Engl. J. Med. **342:**626–633.
37. **Lisztwan, J., G. Imbert, C. Wirbelauer, M. Gstaiger, and W. Krek.** 1999. The von Hippel-Lindau tumor suppressor protein is a component of an E3 ubiquitin-protein ligase activity. Genes Dev. **13:**1822–1833.
38. **Lonser, R. R., G. M. Glenn, M. Walther, E. Y. Chew, S. K. Libutti, W. M. Linehan, and E. H. Oldfield.** 2003. von Hippel-Lindau disease. Lancet **361:**2059–2067.
39. **Ma, W., L. Tessarollo, S. B. Hong, M. Baba, E. Southon, T. C. Back, S. Spence, C. G. Lobe, N. Sharma, G. W. Maher, S. Pack, A. O. Vortmeyer, C. Guo, B. Zbar, and L. S. Schmidt.** 2003. Hepatic vascular tumors, angiectasis in multiple organs, and impaired spermatogenesis in mice with conditional inactivation of the VHL gene. Cancer Res. **63:**5320–5328.
40. **Mack, F. A., W. K. Rathmell, A. M. Arsham, J. Gnarra, B. Keith, and M. C. Simon.** 2003. Loss of pVHL is sufficient to cause HIF dysregulation in primary cells but does not promote tumor growth. Cancer Cell **3:**75–88.
41. **Maynard, M. A., A. J. Evans, T. Hosomi, S. Hara, M. A. Jewett, and M. Ohh.** 2005. Human HIF-3alpha4 is a dominant-negative regulator of HIF-1 and is down-regulated in renal cell carcinoma. FASEB J. **19:**1396–1406.
42. **Minamisawa, S., Y. Gu, J. Ross, Jr., K. R. Chien, and J. Chen.** 1999. A post-transcriptional compensatory pathway in heterozygous ventricular my-

osin light chain 2-deficient mice results in lack of gene dosage effect during normal cardiac growth or hypertrophy. J. Biol. Chem. **274:**10066–10070.
43. **Moreira, P. I., S. L. Siedlak, X. Wang, M. S. Santos, C. R. Oliveira, M. Tabaton, A. Nunomura, L. I. Szweda, G. Aliev, M. A. Smith, X. Zhu, and G. Perry.** 2007. Autophagocytosis of mitochondria is prominent in Alzheimer disease. J. Neuropathol. Exp. Neurol. **66:**525–532.
44. **Ohh, M., R. L. Yauch, K. M. Lonergan, J. M. Whaley, A. O. Stemmer-Rachamimov, D. N. Louis, B. J. Gavin, N. Kley, W. G. Kaelin, Jr., and O. Iliopoulos.** 1998. The von Hippel-Lindau tumor suppressor protein is required for proper assembly of an extracellular fibronectin matrix. Mol. Cell **1:**959–968.
45. **Pennacchietti, S., P. Michieli, M. Galluzzo, M. Mazzone, S. Giordano, and P. M. Comoglio.** 2003. Hypoxia promotes invasive growth by transcriptional activation of the met protooncogene. Cancer Cell **3:**347–361.
46. **Pfander, D., T. Kobayashi, M. C. Knight, E. Zelzer, D. A. Chan, B. R. Olsen, A. J. Giaccia, R. S. Johnson, V. H. Haase, and E. Schipani.** 2004. Deletion of Vhlh in chondrocytes reduces cell proliferation and increases matrix deposition during growth plate development. Development **131:**2497–2508.
47. **Pugh, C. W., and P. J. Ratcliffe.** 2003. The von Hippel-Lindau tumor suppressor, hypoxia-inducible factor-1 (HIF-1) degradation, and cancer pathogenesis. Semin. Cancer Biol. **13:**83–89.
48. **Rajagopalan, S., J. Olin, S. Deitcher, A. Pieczek, J. Laird, P. M. Grossman, C. K. Goldman, K. McEllin, R. Kelly, and N. Chronos.** 2007. Use of a constitutively active hypoxia-inducible factor-1alpha transgene as a therapeutic strategy in no-option critical limb ischemia patients: phase I dose-escalation experience. Circulation **115:**1234–1243.
49. **Rankin, E. B., M. P. Biju, Q. Liu, T. L. Unger, J. Rha, R. S. Johnson, M. C. Simon, B. Keith, and V. H. Haase.** 2007. Hypoxia-inducible factor-2 (HIF-2) regulates hepatic erythropoietin in vivo. J. Clin. Investig. **117:**1068–1077.
50. **Safran, M., and W. G. Kaelin, Jr.** 2003. HIF hydroxylation and the mammalian oxygen-sensing pathway. J. Clin. Investig. **111:**779–783.
51. **Semenza, G. L.** 2001. HIF-1 and mechanisms of hypoxia sensing. Curr. Opin. Cell Biol. **13:**167–171.
52. **Semenza, G. L.** 2001. HIF-1, O(2), and the 3 PHDs: how animal cells signal hypoxia to the nucleus. Cell **107:**1–3.
53. **Sharma, S., J. V. Adrogue, L. Golfman, I. Uray, J. Lemm, K. Youker, G. P. Noon, O. H. Frazier, and H. Taegtmeyer.** 2004. Intramyocardial lipid accumulation in the failing human heart resembles the lipotoxic rat heart. FASEB J. **18:**1692–1700.
54. **Sharp, R., J. A. Recio, C. Jhappan, T. Otsuka, S. Liu, Y. Yu, W. Liu, M. Anver, F. Navid, L. J. Helman, R. A. DePinho, and G. Merlino.** 2002. Synergism between INK4a/ARF inactivation and aberrant HGF/SF signaling in rhabdomyosarcomagenesis. Nat. Med. **8:**1276–1280.
55. **Takagi, H., Y. Matsui, S. Hirotani, H. Sakoda, T. Asano, and J. Sadoshima.** 2007. AMPK mediates autophagy during myocardial ischemia in vivo. Autophagy **3:**405–407.
56. **Tanaka, H., M. Yamamoto, N. Hashimoto, M. Miyakoshi, S. Tamakawa, M. Yoshie, Y. Tokusashi, K. Yokoyama, Y. Yaginuma, and K. Ogawa.** 2006. Hypoxia-independent overexpression of hypoxia-inducible factor 1alpha as an early change in mouse hepatocarcinogenesis. Cancer Res. **66:**11263–11270.
57. **Tang, N., L. Wang, J. Esko, F. J. Giordano, Y. Huang, H. P. Gerber, N. Ferrara, and R. S. Johnson.** 2004. Loss of HIF-1alpha in endothelial cells disrupts a hypoxia-driven VEGF autocrine loop necessary for tumorigenesis. Cancer Cell **6:**485–495.
58. **Thomas, W. G., Y. Brandenburger, D. J. Autelitano, T. Pham, H. Qian, and R. D. Hannan.** 2002. Adenoviral-directed expression of the type 1A angiotensin receptor promotes cardiomyocyte hypertrophy via transactivation of the epidermal growth factor receptor. Circ. Res. **90:**135–142.
59. **Tracy, K., B. C. Dibling, B. T. Spike, J. R. Knabb, P. Schumacker, and K. F. Macleod.** 2007. BNIP3 is an RB/E2F target gene required for hypoxia-induced autophagy. Mol. Cell. Biol. **27:**6229–6242.
60. **Vincent, K. A., K. G. Shyu, Y. Luo, M. Magner, R. A. Tio, C. Jiang, M. A. Goldberg, G. Y. Akita, R. J. Gregory, and J. M. Isner.** 2000. Angiogenesis is induced in a rabbit model of hindlimb ischemia by naked DNA encoding an HIF-1alpha/VP16 hybrid transcription factor. Circulation **102:**2255–2261.
61. **Yokoyama, T., Y. Kondo, and S. Kondo.** 2007. Roles of mTOR and STAT3 in autophagy induced by telomere 3′ overhang-specific DNA oligonucleotides. Autophagy **3:**496–498.
62. **Yu, F., S. B. White, Q. Zhao, and F. S. Lee.** 2001. HIF-1alpha binding to VHL is regulated by stimulus-sensitive proline hydroxylation. Proc. Natl. Acad. Sci. USA **98:**9630–9635.
63. **Zheng, L., J. Marcusson, and A. Terman.** 2006. Oxidative stress and Alzheimer disease: the autophagy connection? Autophagy **2:**143–145.
64. **Zhu, H., P. Tannous, J. L. Johnstone, Y. Kong, J. M. Shelton, J. A. Richardson, V. Le, B. Levine, B. A. Rothermel, and J. A. Hill.** 2007. Cardiac autophagy is a maladaptive response to hemodynamic stress. J. Clin. Investig. **117:**1782–1793.